

THE EFFECT OF THE LABORATORY SPECIMEN ON FATIGUE CRACK GROWTH RATE

Forth, S.C.^{1*}, Johnston, W.M.², Seshadri, B.R.³

¹NASA Langley Research Center

²Lockheed Martin Corporation

³National Institute of Aerospace

*2 West Reid Street, MS 188E

Hampton, VA 23681 USA

Scott.C.Forth@nasa.gov

ABSTRACT

Over the past thirty years, laboratory experiments have been devised to develop fatigue crack growth rate data that is representative of the material response. The crack growth rate data generated in the laboratory is then used to predict the safe operating envelope of a structure. The ability to interrelate laboratory data and structural response is called similitude. In essence, a nondimensional term, called the stress intensity factor, was developed that includes the applied stresses, crack size and geometric configuration. The stress intensity factor is then directly related to the rate at which cracks propagate in a material, resulting in the material property of fatigue crack growth response. Standardized specimen configurations and experimental procedures have been developed for laboratory testing to generate crack growth rate data that supports similitude of the stress intensity factor solution. In this paper, the authors present laboratory fatigue crack growth rate test data and finite element analyses that show similitude between standard specimen configurations tested using the constant stress ratio test method is unobtainable.

Introduction

One of the responses of a material to extreme forces, such as stress, temperature, etc., is to crack. A crack appears when the material reaches a limit in its capability to absorb damage and fails. Sometimes, a crack will grow under a periodically applied condition, such as cyclic loading, that are well below the stresses required to fail the material, denoted fatigue crack growth. Over the past thirty years, laboratory experiments have been devised to develop fatigue crack growth rate data that is representative of the material response. The crack growth rate data generated in the laboratory is then used to predict the safe operating envelope of a structure. The ability to interrelate laboratory data and structural response is called similitude. In essence, a nondimensional term, called the stress intensity factor, was developed that includes the applied stresses, crack size and geometric configuration. The stress intensity factor is then directly related to the rate at which cracks propagate in a material, resulting in the material property of fatigue crack growth response.

Standardized specimen configurations have been developed for laboratory testing to generate crack growth rate data that supports similitude of the stress intensity factor solution. Recent research into fatigue crack growth rate data has exposed some limitations in the testing standards [1, 2]. The typical approach to generate crack growth rate data at a specific stress-ratio is accomplished by reducing both the maximum and minimum applied load at a specific rate until the crack arrests. Several researchers [3 - 6] have all postulated that a constant stress ratio load reduction method produces results that are not representative of the material behavior but an artifact of the laboratory environment. Furthermore, Liknes and Stephens [7] and Garr and Hresko [8] have suggested that specimen configurations contained within the standards can have an effect on threshold by influencing extrinsic closure affects. The middle crack tension, compact tension and eccentrically loaded edge-crack tension specimen configurations are widely used for generating fatigue crack growth rate data [9]. In this paper, the authors present laboratory fatigue crack growth rate data generated using the standard constant stress ratio load reduction method that is specimen dependent and does not support similitude.

Experimental Method

Fatigue crack growth rate data for D6AC steel is presented in this paper that is dependent on specimen configuration. The steel alloy D6AC was chosen for study because it is used extensively by the aerospace industry [9]. Constant stress ratio, R , of 0.1 and maximum stress intensity factor range, K_{max} , of 22 MPa $m^{1/2}$ fatigue crack growth rate data was generated using four different compact tension, C(T), specimen configurations ($W = 76.2$ mm, $B = 12.7$ mm, $W = 76.2$ mm, $B = 5.08$ mm, $W =$

50.8 mm, $B = 5.08$ mm, and $W = 25.4$ mm, $B = 5.08$ mm), one eccentrically-loaded side edge tension, ESE(T), specimen configuration ($W = 38.1$ mm, $B = 5.08$ mm), and two middle tension, M(T), specimen configurations ($W = 76.2$ mm, $B = 12.7$ mm, and $W = 76.2$ mm, $B = 5.08$ mm). The laboratory environment, denoted “room temp, lab air” varies between room temperatures of 20° to 30° C, with a mean of 23° C, and the laboratory air relative humidity varies between 24 to 38%, with a mean of 28%. All experiments were conducted in loading frames of 89 to 222 kilonewton capacity. Load range cards were used to improve resolution for lower applied forces to within 2% of the expected force. The tests were conducted in force control at a frequency of 20 Hz using an analog controller. A computer control system [10] was used for K control of the C(T) specimens to adjust the forces based on compliance readings from strain or displacement gages and user input. Visual measurements of the crack length were taken throughout the test to verify the compliance based crack length used to control the test system. The M(T) specimens were installed in hydraulically actuated wedge grips and force was shed manually using the step method described in ASTM E 647. The C(T) and ESE(T) specimens were installed in sized clevises for each width tested and force was shed using K control at a rate of -80/m. A minimum of one repeat was performed for all test conditions presented. The scatter was less than 10% on ΔK for any given growth rate, da/dN for all conditions tested.

Computational Method

Three-dimensional finite element analyses of both the C(T) and M(T) were analyzed using the ZIP3D [11] finite element code. ZIP3D is an elastic-plastic material, non-linear finite element software with capabilities to carryout fatigue and fracture analysis. A typical detail of a ZIP3D finite element model along with a schematic of the C(T) specimen are shown in Figure 1. The C(T) was modeled with a thickness $B = 12.7$ mm and width $W = 50.8$, and an initial crack length to width ratio, $a/W = 0.25$. The analysis has not been conducted on the tested ductile steel, D6AC, but the trends in crack opening displacement presented herein should be similar. The material considered throughout the analyses was aluminum alloy 7075-T73. The material was assumed to have a bi-linear character with modulus $E = 71.0$ GPa and flow stress $\sigma_o = 400$ MPa. The von Mises yield criterion and the associated flow rule were used. Small deformation theory was employed. The load cycles were applied to simulate load reduction from as high a ΔK of 30 MPa \sqrt{m} all the way to 1 MPa \sqrt{m} under both constant R and constant K_{max} load reduction procedures. The crack front and load were adjusted during each analysis step such that $da = 10$ microns (one element size). Complete information on these analyses can be found in Seshadri and Forth [12].

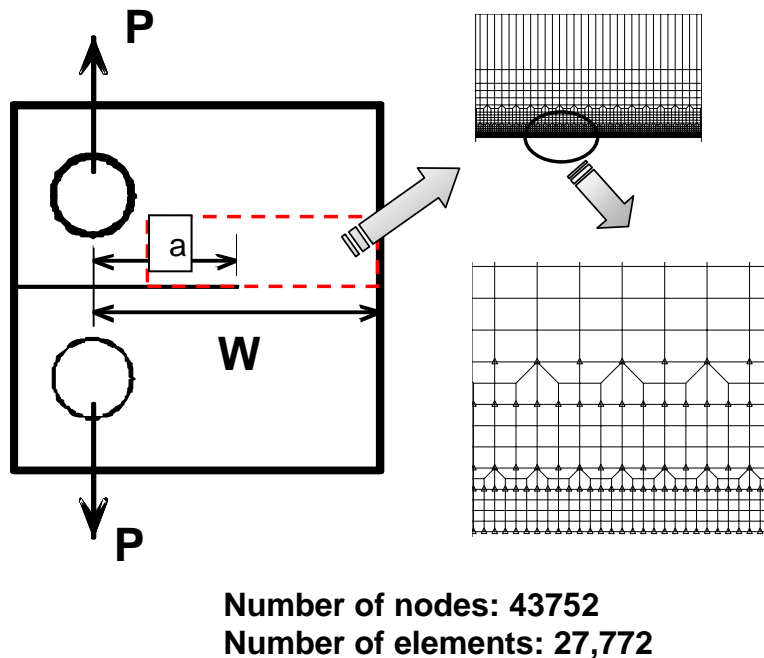


Figure 1— A typical ZIP3d finite element model of C(T) specimen.

Constant Stress Ratio Load Reduction

Crack growth rate data was generated using M(T) and C(T) specimens of varying thicknesses and widths at a stress ratio, R, of 0.1. Figure 1 plots crack growth rate, da/dN , versus stress intensity factor range, ΔK , for a stress ratio, $R = 0.1$, condition omitting the 50.8 and 25.4 mm wide C(T) specimen data. The differences in crack growth rate data between the specimen configurations presented in Figure 1 are large as the growth rate drops below 10^{-8} meters/cycle. The divergence of the specimen data occurs because some of the specimens are developing environmental- and roughness-induced fretting-oxide

debris crack closure that retards the crack [5]. Photographs of representative fracture surfaces for the 5.08 and 12.7 mm thick C(T) specimens are shown in Figure 3 to illustrate the development of fretting-oxide debris on the 12.7 mm thick C(T) specimen fracture surfaces (Figure 3a). The 5.08 mm thick C(T), as shown in Figure 3b, M(T) and ESE(T) specimens do not develop oxide debris on the fracture surface at the humidity levels seen in laboratory air [13]. A comparison of the local cyclic CTOD and crack closure levels for M(T) and C(T) specimens computed in the finite element analyses is shown in Figure 4. The black and red lines show variation in cyclic CTOD across the thickness with applied ΔK for M(T) and C(T) specimens respectively. The blue and green lines represent variation in closure level across the thickness for M(T) and C(T) specimens. From the beginning of the constant R load reduction procedure, the estimated cyclic CTOD values across the thickness for M(T) specimen are within the bounds of C(T) specimen. That means to say that at any applied ΔK during the constant R load reduction procedure, the estimated local cyclic CTOD at any location across the thickness of M(T) specimen is a few percent less than the corresponding C(T) specimen. Also, during the initial part of the constant R load reduction procedure, the M(T) specimen has higher local crack closure level across the thickness when compared to the C(T) specimen. However, once the applied ΔK reduces below $6 \text{ MPa}\sqrt{\text{m}}$, locally the crack remains fully open for both specimen types. In general, during the constant R load reduction procedure, both M(T) and C(T) specimens have similar local cyclic CTOD behavior. Therefore, the crack growth rate behavior shown in Figure 2 is not a function of plasticity-induced crack closure, but of a specimen configuration susceptibility to the development of fretting-oxide debris under the constant R = 0.1 load reduction test method.

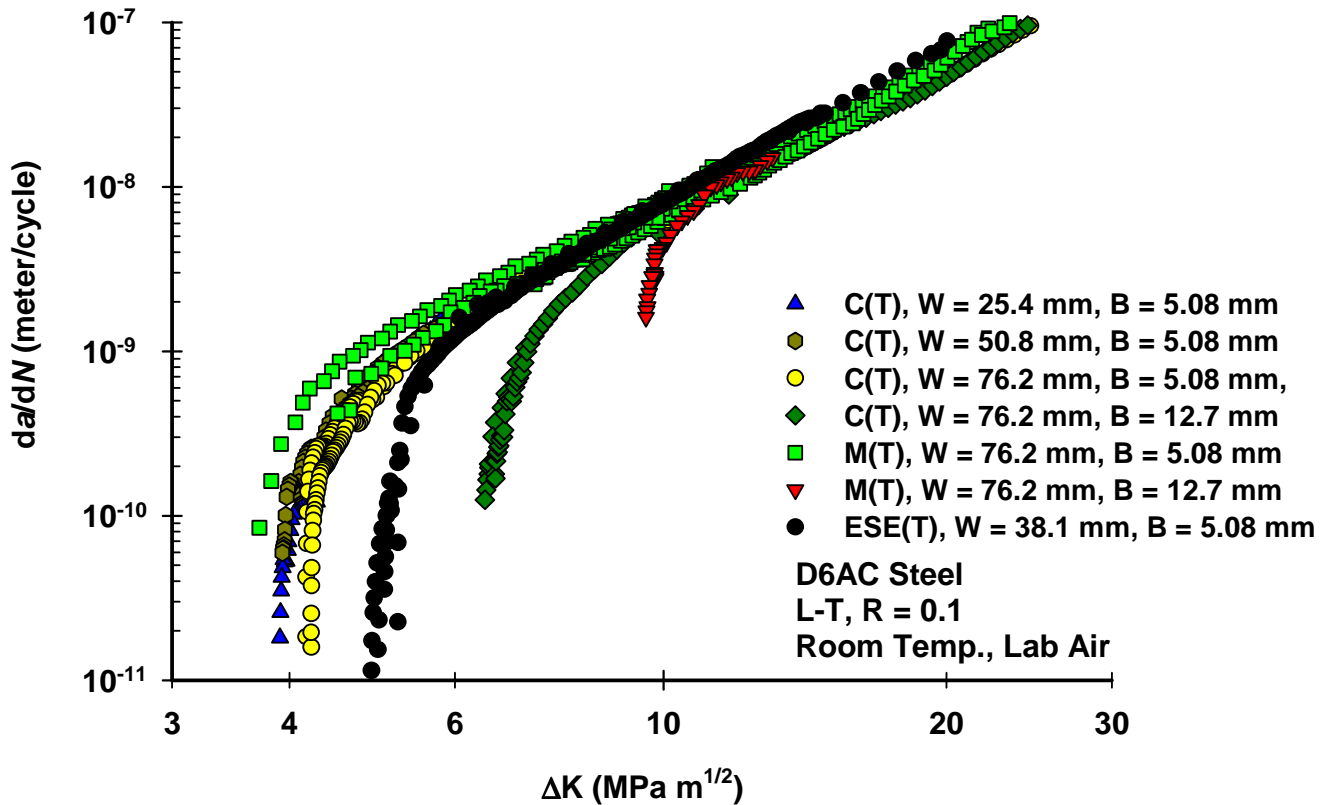


Figure 2— Crack growth rate versus stress intensity factor range at R = 0.1 for different specimen configurations.



Figure 3— Photographs of representative fracture surfaces for C(T) specimens in lab air: (a) 76.2 mm wide, 12.7 mm thick; (b) 76.2 mm wide, 5.08 mm thick.

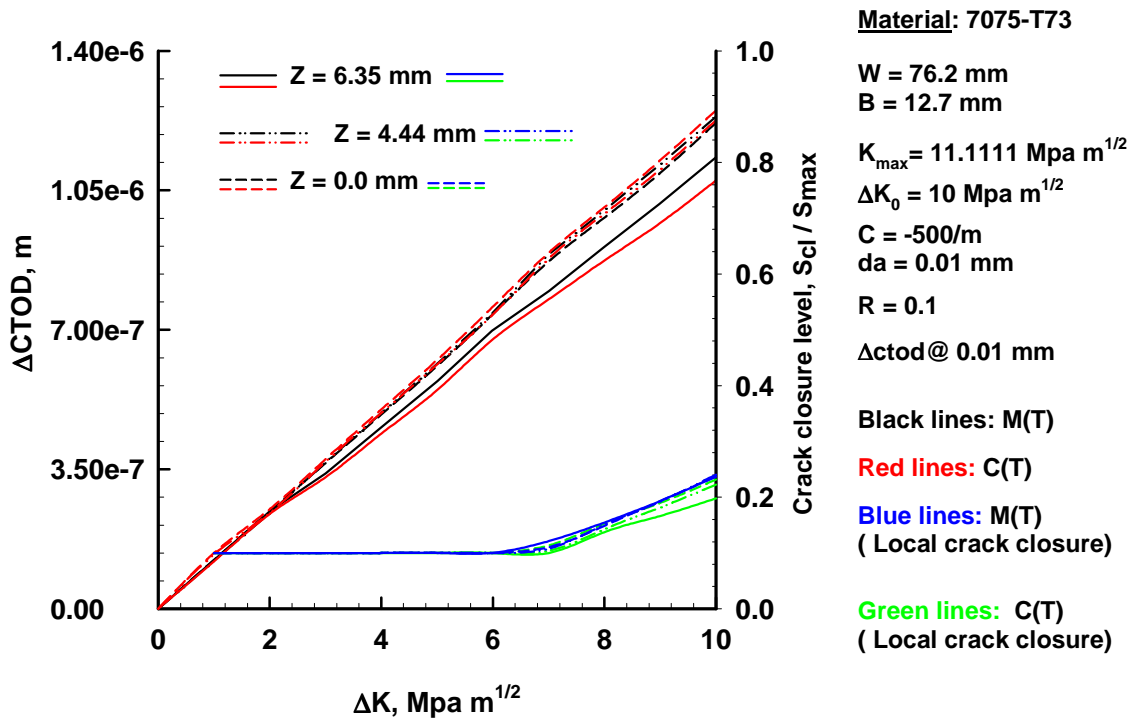


Figure 4— Comparison of variation in local $\Delta CTOD$ with applied constant-R load reduction procedure for C(T) and M(T) specimens.

Constant K_{max} Load Reduction

Constant $K_{max} = 22 \text{ MPa m}^{1/2}$ tests were performed to develop crack growth rate data that has minimal influence from extrinsic effects, such as the environmental- and roughness-induced crack closure depicted in Figure 3a. The constant K_{max} crack growth rate data plotted in Figure 5 shows that for any value of ΔK , there is little difference between any of specimen configurations. The lack of sensitivity of the K_{max} test data to specimen configuration implies that the extrinsic effects, such as crack closure that can develop in a constant $R = 0.1$ load reduction test, have different effects on different specimen configurations. Comparison of local cyclic CTOD and crack closure levels for M(T) and C(T) specimens computed using the finite element method under the constant K_{max} load reduction procedure are shown in Figure 6. Once again, the black and red lines show variation in cyclic CTOD across the thickness with applied ΔK for M(T) and C(T) specimens respectively. The closure levels are not shown because crack closure is approximately zero in a constant K_{max} test. At any given applied ΔK during the load reduction procedure, the cyclic CTOD estimate for the C(T) is greater than the M(T) specimen. However, the difference in the magnitude of the CTOD across the specimen thickness is small. Since the constant K_{max} test procedure develops crack growth rate data that is independent of specimen configuration, it is representative of a material response, and provides a baseline of data to support similitude, *i.e.* the data can be used to predict the response of different structural configurations.

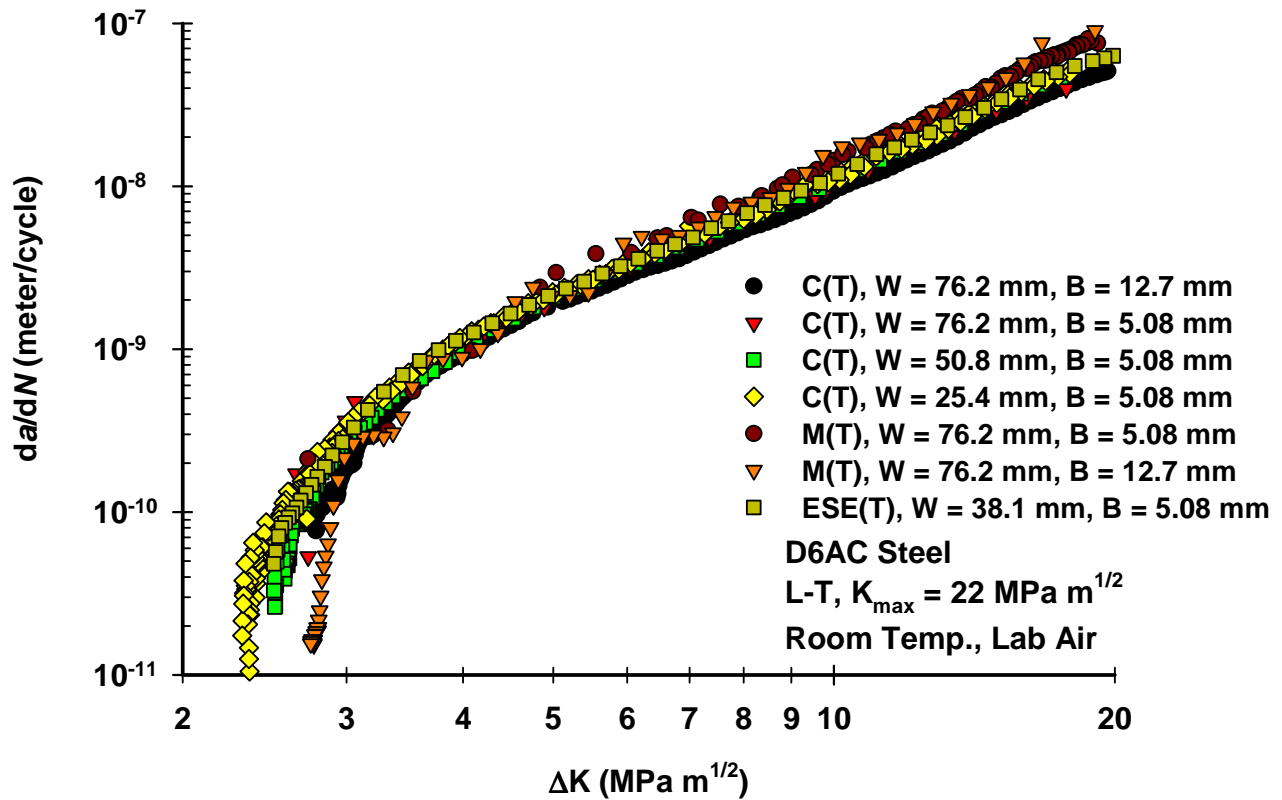


Figure 5— Crack growth rate versus stress intensity factor range data for $K_{max} = 22 \text{ MPa m}^{1/2}$ in lab air.

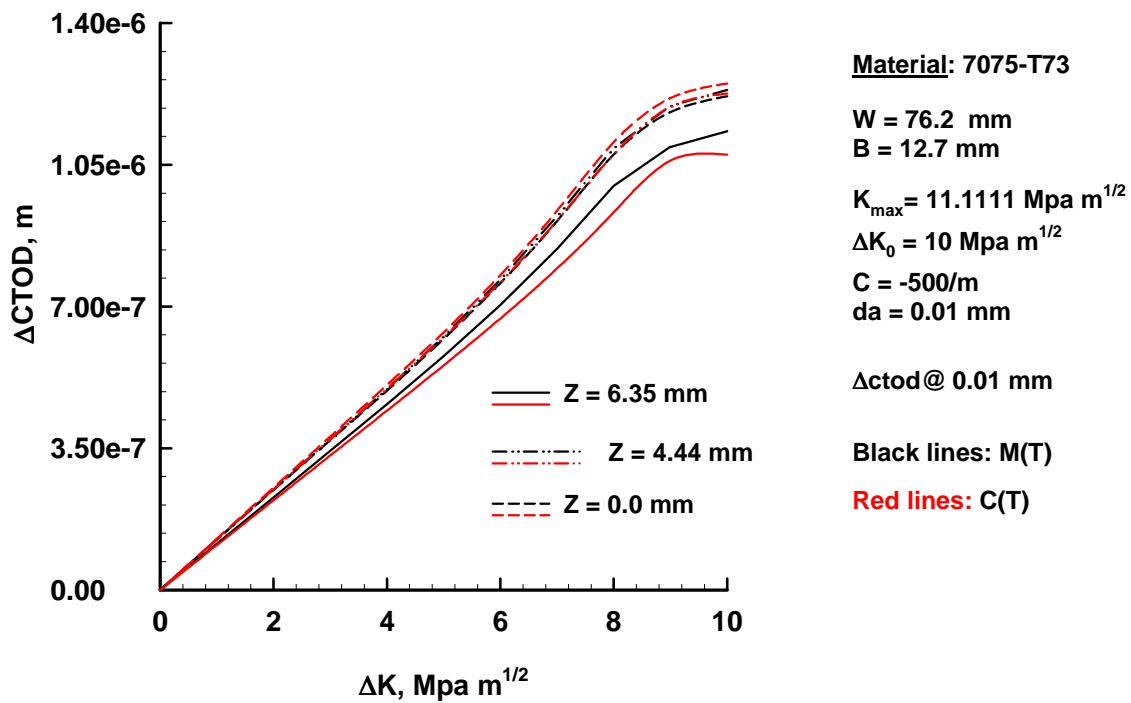


Figure 6— Comparison of variation in local $\Delta CTOD$ with applied constant- K_{max} load reduction procedure for C(T) and M(T) specimens.

Summary

Fatigue crack growth rate data was generated and modeled using several different standard specimen configurations. The data was generated using two experimental procedures that have been standardized with the intent of generating fatigue crack growth rate data that supports the theory of similitude. In other words, the fatigue crack growth rate data generated with either the constant stress ratio or K_{max} procedure is purported to be representative of a material response that can be applied to any structural analysis. However, tests conducted with the constant stress ratio load reduction procedure generated results that were dependent on the specimen configuration (Figure 2) contrary to the finite element model (Figure 4). The finite element model captures the effects of plasticity on crack growth and clearly shows in Figure 4 that crack growth rate is specimen independent. Therefore, the data presented in Figure 2 is principally affected by other forms of closure not modeled by the finite element analyses, such as environment and roughness. The data generated using the constant stress ratio load reduction test is only useful for understanding the behavior of a crack in a C(T), ESE(T) or M(T) specimen under the specific loading and environmental conditions. To extrapolate the fatigue crack growth response presented in Figure 2 to predict the response of a structural component would be unwise and potentially catastrophic. For it is unknown if the data presented in Figure 2 is conservative with respect to the response of a structure. In contrast, both the fatigue crack growth rate data (Figure 5) and finite element analyses (Figure 6) generated using the constant K_{max} test procedure were insensitive to the specimen configuration. Figure 7 is a plot of the fatigue crack growth threshold (where $da/dN \sim 10^{-10}$ meters/cycle) versus stress ratio that clearly shows the threshold data generated using the constant $R = 0.1$ procedure varies from 3.5 to 9.76 MPa $m^{1/2}$ dependent on specimen configuration, whereas the constant K_{max} test procedure varies from 2.62 to 3.02 MPa $m^{1/2}$. In summary, the constant stress ratio test data presented in this paper is not representative of similitude contrary to the finite element analyses and is therefore not useful in predicting the response of any other structural configuration.

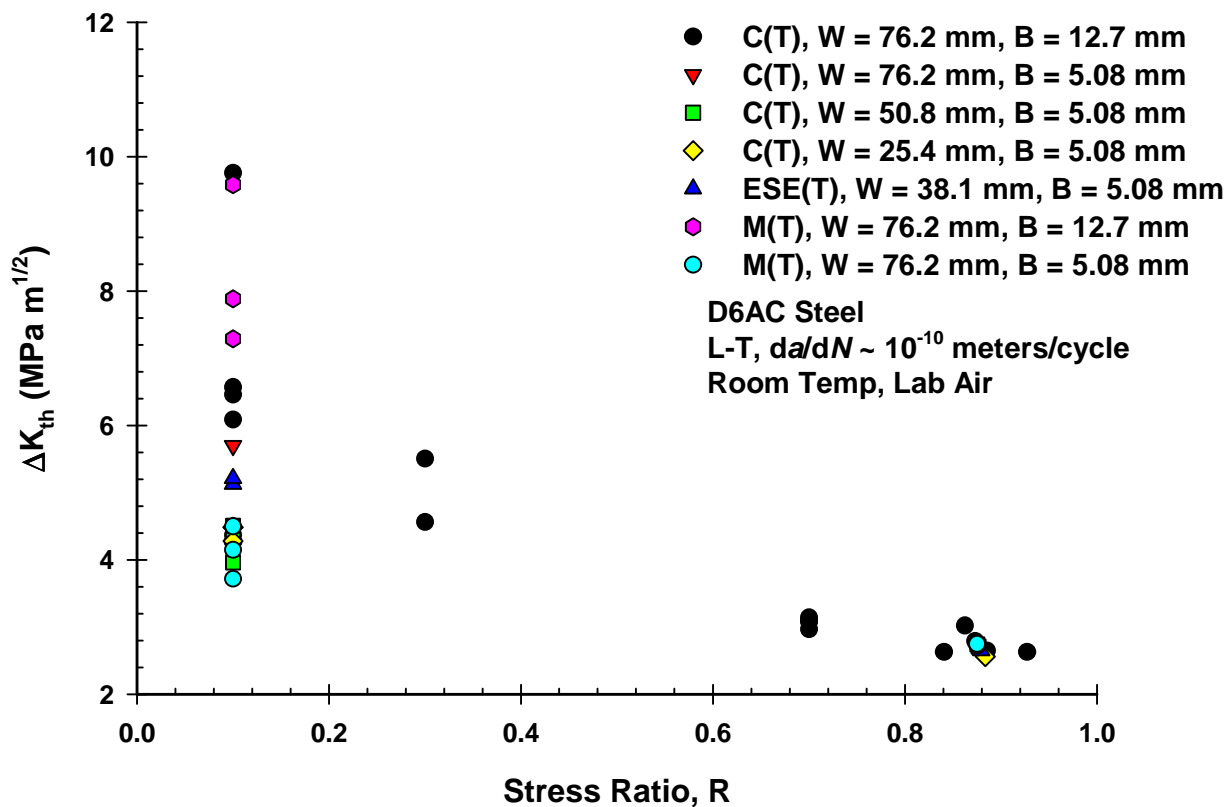
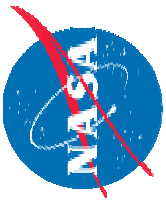


Figure 7— Stress intensity factor range at $da/dN \sim 10^{-10}$ meters/cycle versus stress ratio.

Reference

1. Tabernig, B., Powell, P. and Pippan, R., Fatigue Crack Growth Thresholds, Endurance Limits, and Design, ASTM STP 1372, ASTM, 96-108, 2000.
2. Newman, J.C., Jr., Fatigue Crack Growth Thresholds, Endurance Limits, and Design, ASTM STP 1372, ASTM, 227-251, 2000.
3. Pippan, R., Stuwe, H.P. and Golos, K., International Journal of Fatigue, **16**, 579-582, 1994.

4. Smith, S.W. and R.S. Piascik, Fatigue Crack Growth Thresholds, Endurance Limits, and Design, ASTM STP 1372, ASTM, 109-122, 2000.
5. Suresh, S. and Ritchie, R.O., Engineering Fracture Mechanics, **18**, 4, 785-800, 1983.
6. Forth, S.C., Newman, Jr., J.C. and Forman, R.G., International Journal of Fatigue, **25**, 1, 9-15, 2003.
7. Liknes, H.O. and Stephens, R.R., Fatigue Crack Growth Thresholds, Endurance Limits, and Design, ASTM STP 1372, ASTM, 175-191, 2000.
8. Garr, K.R. and Hresko, G.C., Fatigue Crack Growth Thresholds, Endurance Limits, and Design, ASTM STP 1372, ASTM, 155-174, 2000.
9. Liaw, P.K., Peck, M.G. and Rudd, G.E., Engineering Fracture Mechanics, **43**, 379-400, 1992.
10. Fracture Technology Associates, www.fracturetech.com.
11. Shivakumar, K.N. and Newman Jr., J.C., NASA TM 102753, National Aeronautics and Space Administration, Washington, DC, 1990.
12. Seshadri, B.R., and Forth, S.C., Journal of ASTM International, 2006.
13. Forth, S.C., Newman, J.C., Jr., and Forman, R.G., Journal of ASTM International, **3**, 3, 2006.



The Effect of the Laboratory Specimen on Fatigue Crack Growth Rate

Scott Forth

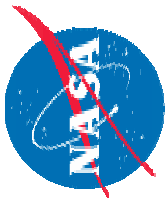
NASA Johnson Space Center

William Johnston

Lockheed Martin Corporation

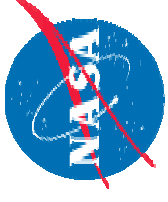
Banavara Seshadri

National Institute for Aerospace



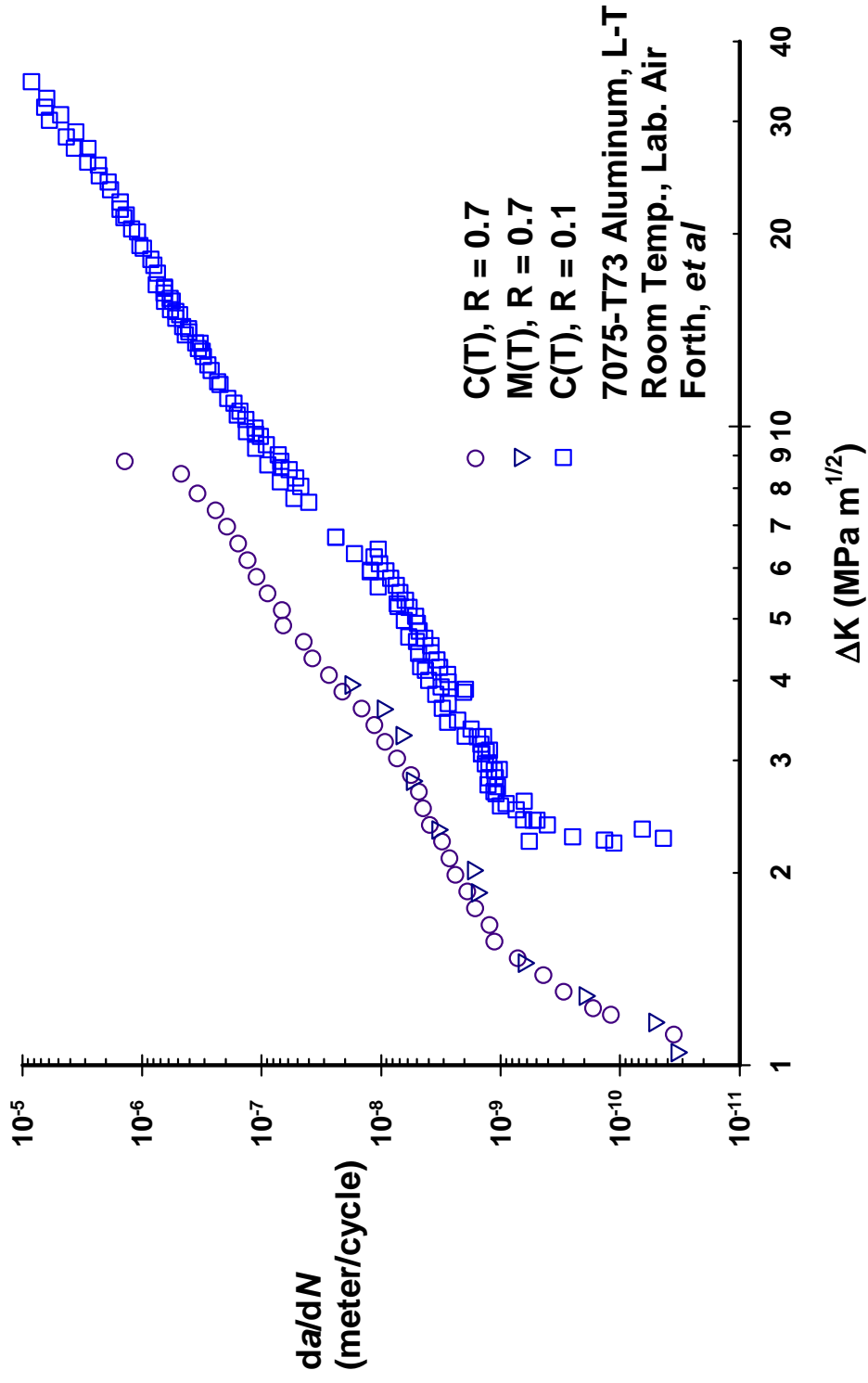
Overview

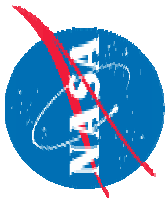
- **Background**
- **Laboratory Test Methods**
- **Computational Method**
- **Experimental Data**
- **Observations**
- **Key Findings**



Background

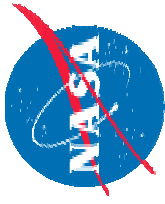
“Typical” Crack Growth Rate Data



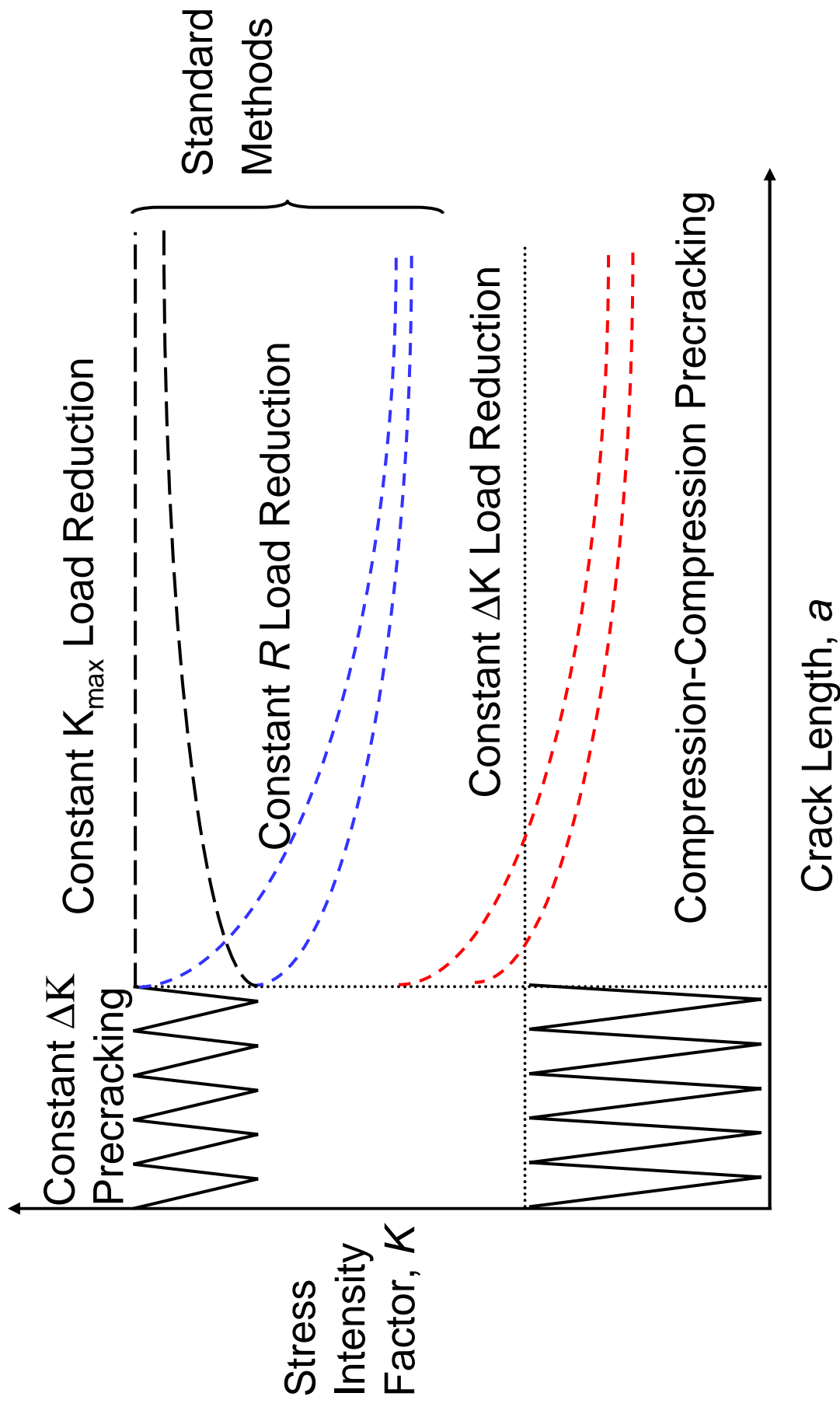


Laboratory Test Methods

- Constant $R = 0.1$ Load Reduction
 - $C = - 50.8$ /mm
 - $\Delta K_i \sim 15$ MPa $m^{1/2}$
- Constant K_{max} Load Reduction
 - $K_{max} = 22$ MPa $m^{1/2}$
 - $C = - 254$ /mm
 - $\Delta K_i \sim 18$ MPa $m^{1/2}$
- Compression Precracking
 - $\Delta K_C \sim 30$ MPa $m^{1/2}$
 - 100,000 cycles
 - $\Delta K_T \sim 7$ MPa $m^{1/2}$
- Specimen Configurations
 - Compact tension, C(T)
 - $W = 76.2$ mm, $B = 12.7$ mm
 - $W = 76.2$ mm, $B = 5.08$ mm
 - $W = 50.8$ mm, $B = 5.08$ mm
 - $W = 25.4$ mm, $B = 5.08$ mm
 - Middle-crack tension, M(T)
 - $W = 76.2$ mm, $B = 12.7$ mm
 - $W = 76.2$ mm, $B = 5.08$ mm
 - Environment
 - 20 – 30 deg. Celsius
 - Lab Air: 20 – 60% RH
 - Dry Air: < 3% RH

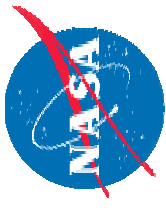


Laboratory Test Methods Cont'

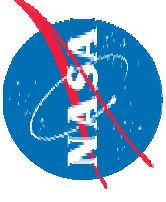


Computational Method

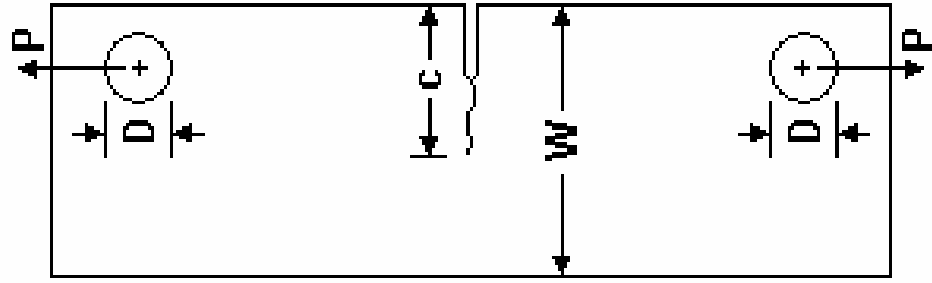
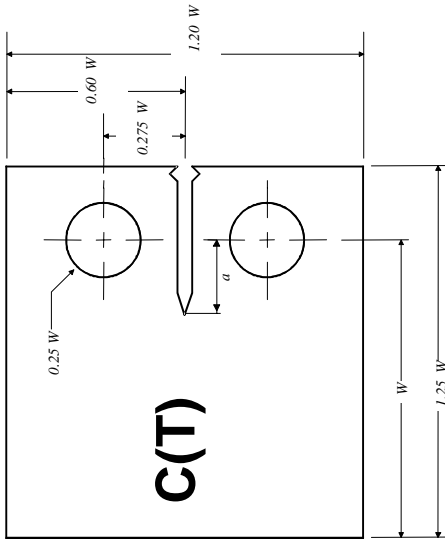
ZIP3D



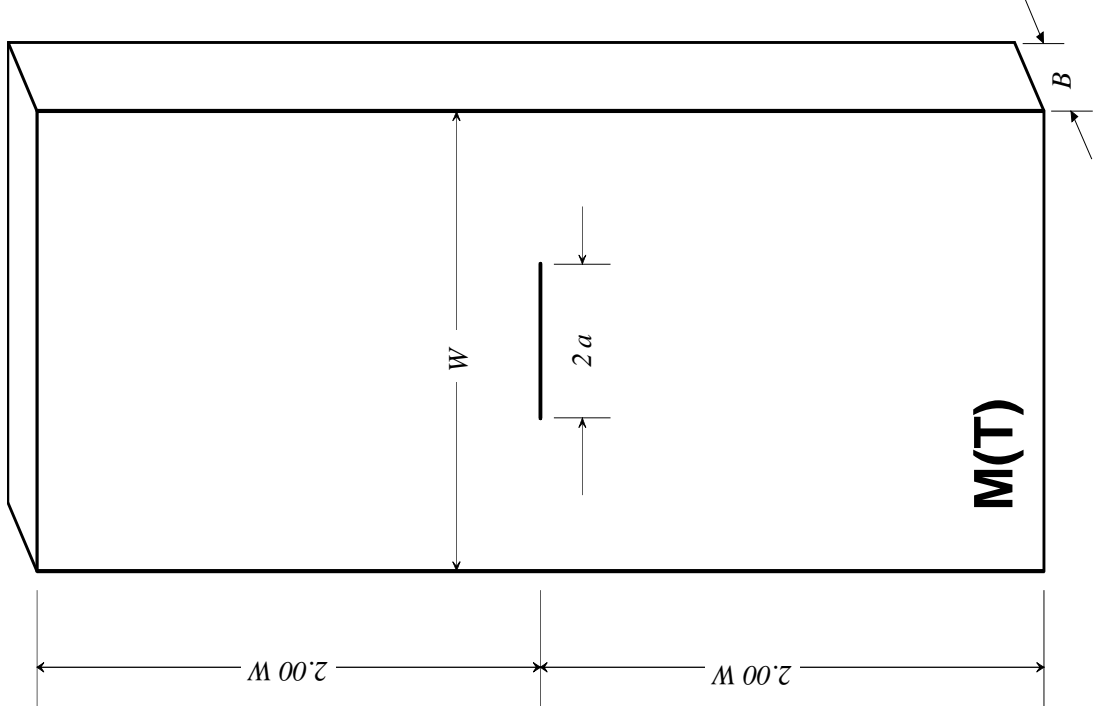
- Elastic-plastic non-linear finite element code
- Element type: Brick element
- Material non-linearity: Elastic-perfectly plastic, Bilinear or Ramberg-Osgood
- Hardening : Isotropic
- Fatigue and Fracture:
 - Cyclic crack growth and crack closure simulations;
 - Evaluation of fracture parameters K and J
 - Stable crack growth using CTOA parameter

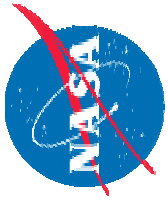


Specimen Configurations

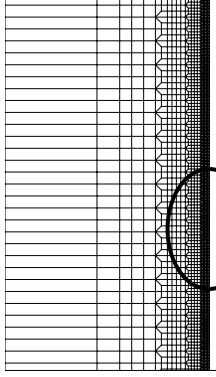
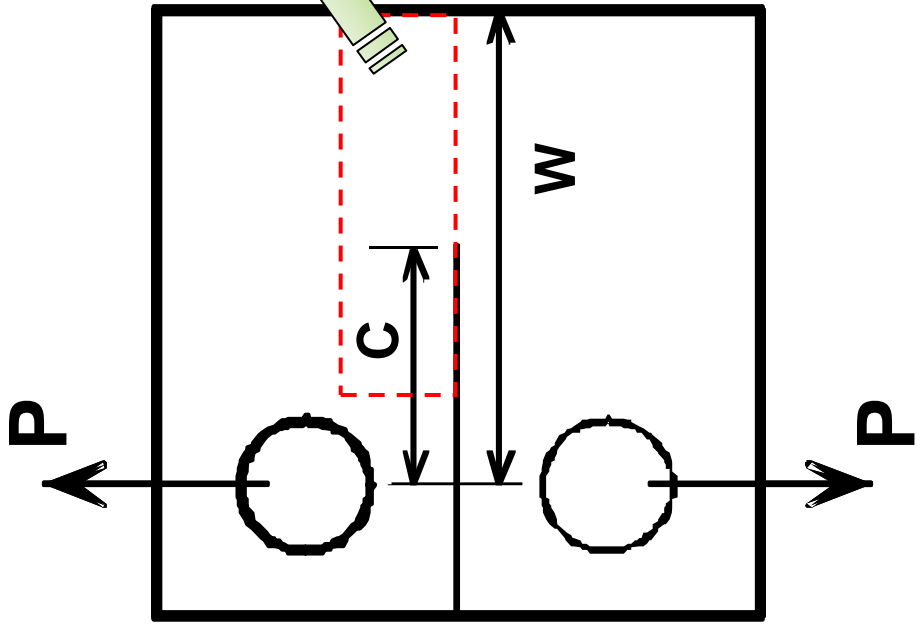


ESE(T)

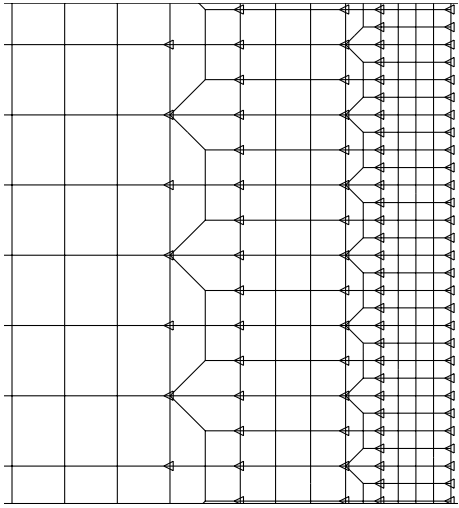


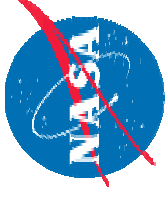


Typical ZIP3D Finite Element Model of C(T) Specimen

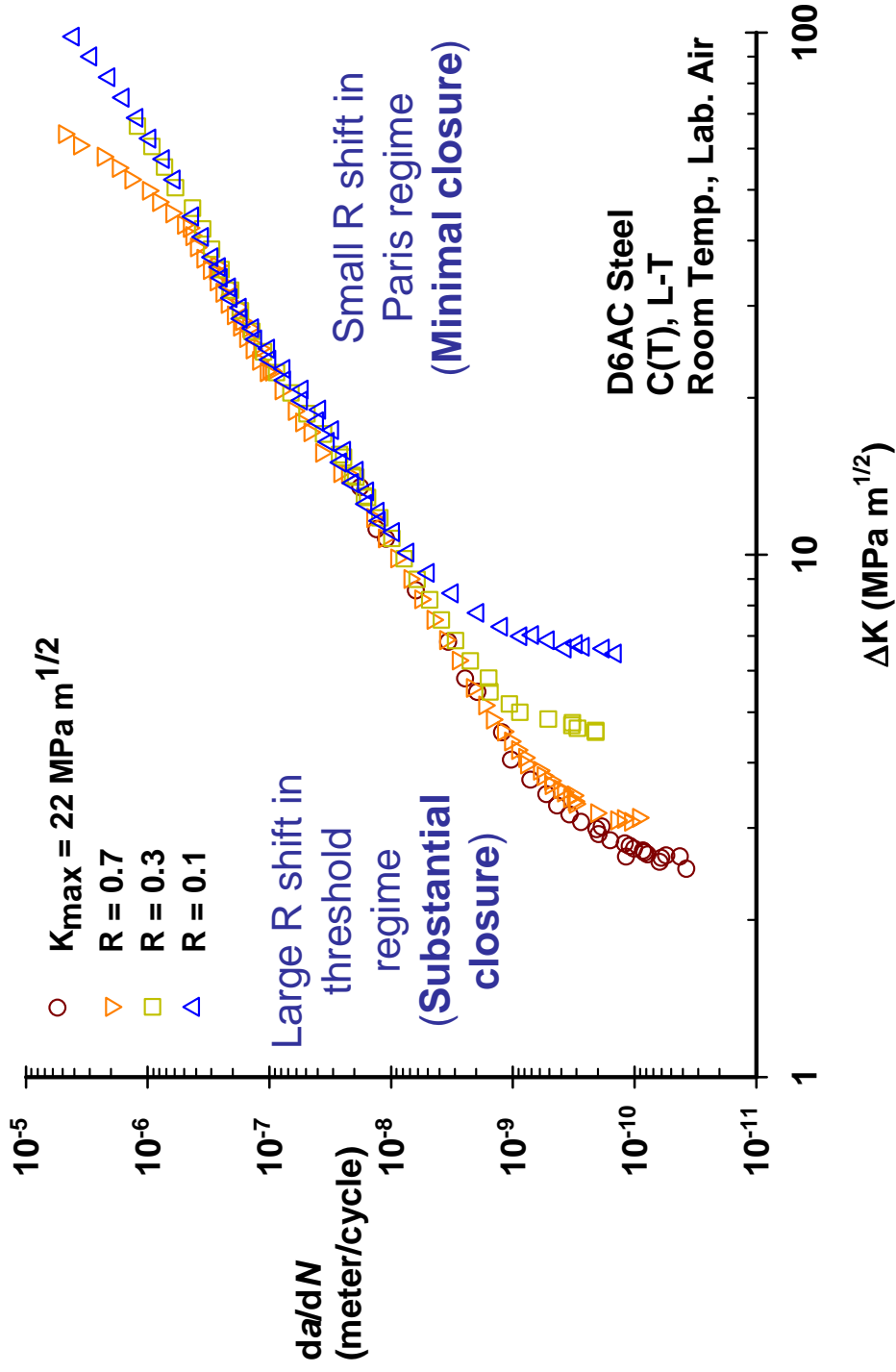


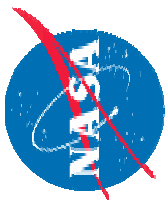
Number of nodes: 43752
Number of elements: 27,772





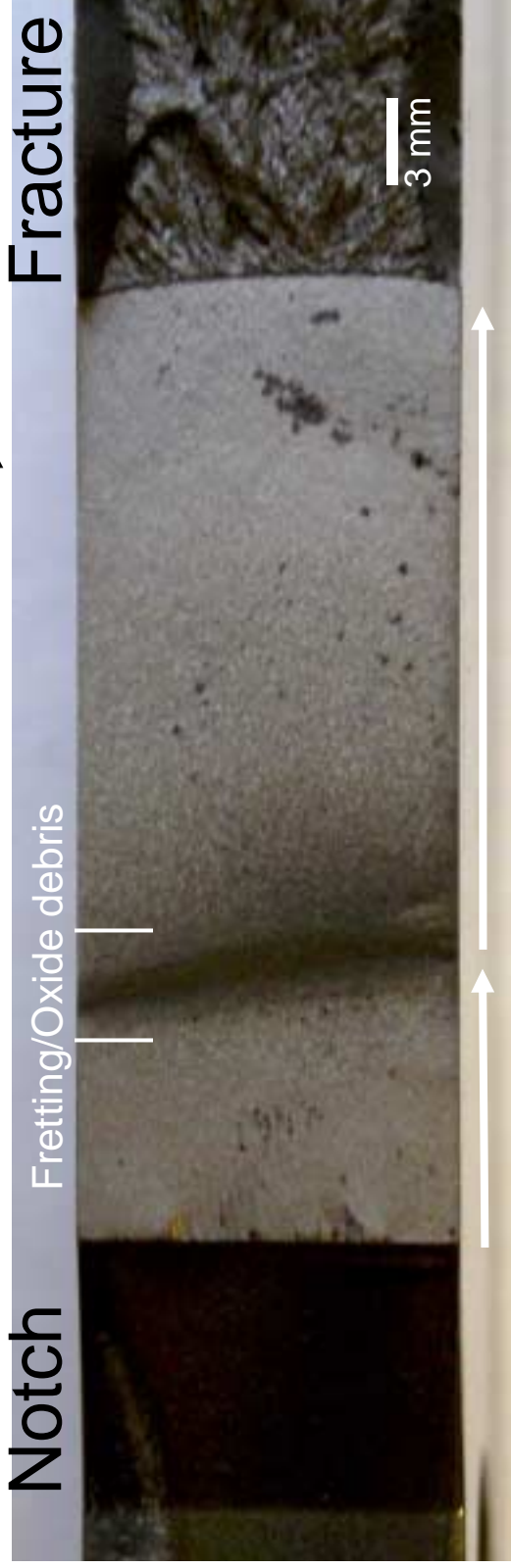
D6AC Crack Growth Rate Data





Evaluation Of $R = 0.1$ Fracture Surface

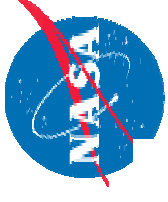
Direction of crack growth 



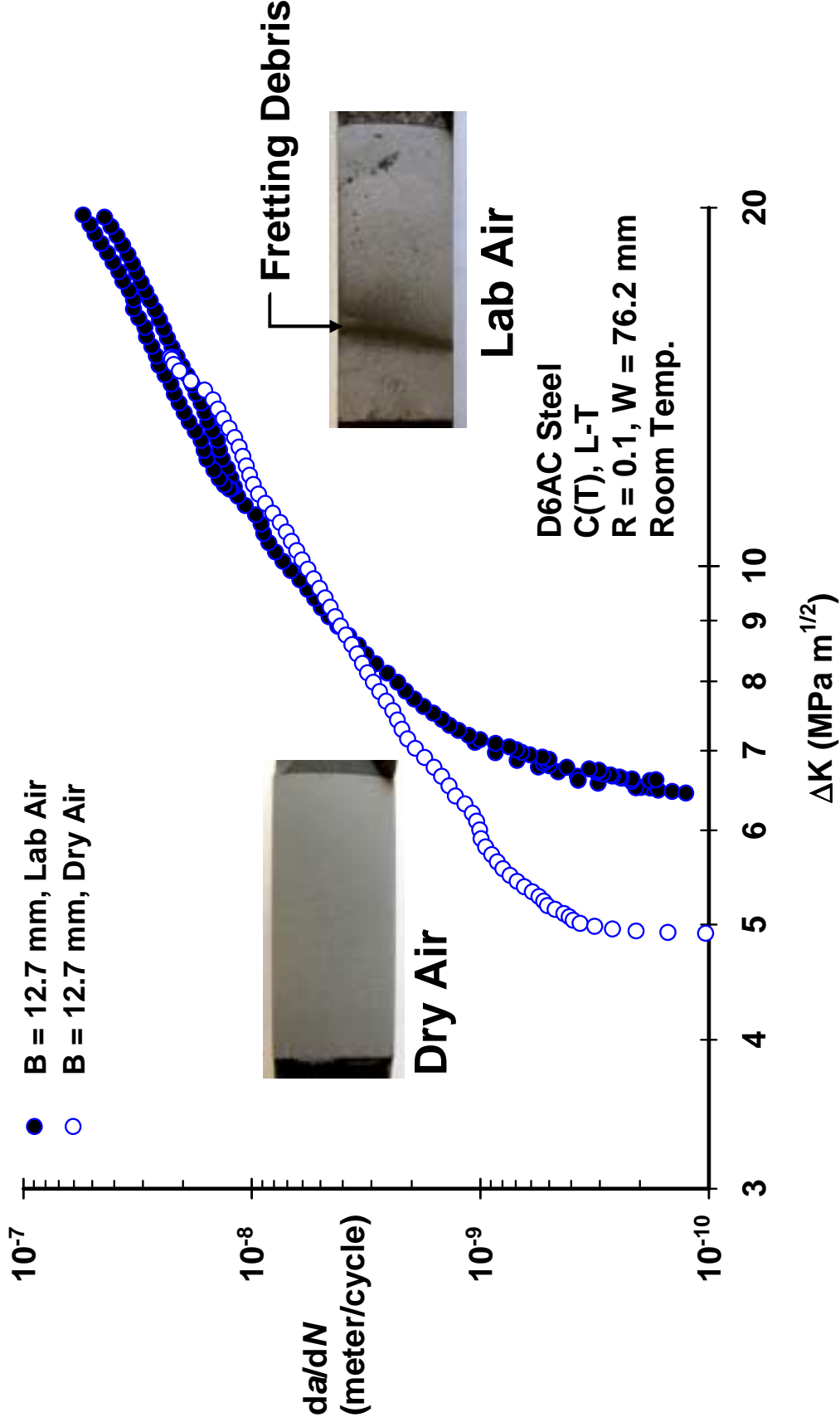
ΔK decreasing ΔK increasing

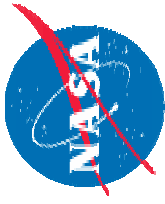
- Interpretation

- Threshold region appears darker in ΔK decreasing test
- As ΔK approaches $10 \text{ MPa m}^{1/2}$ in ΔK increasing test, fracture surface lightens and crack growth rate is equivalent to high-R “closure free” data

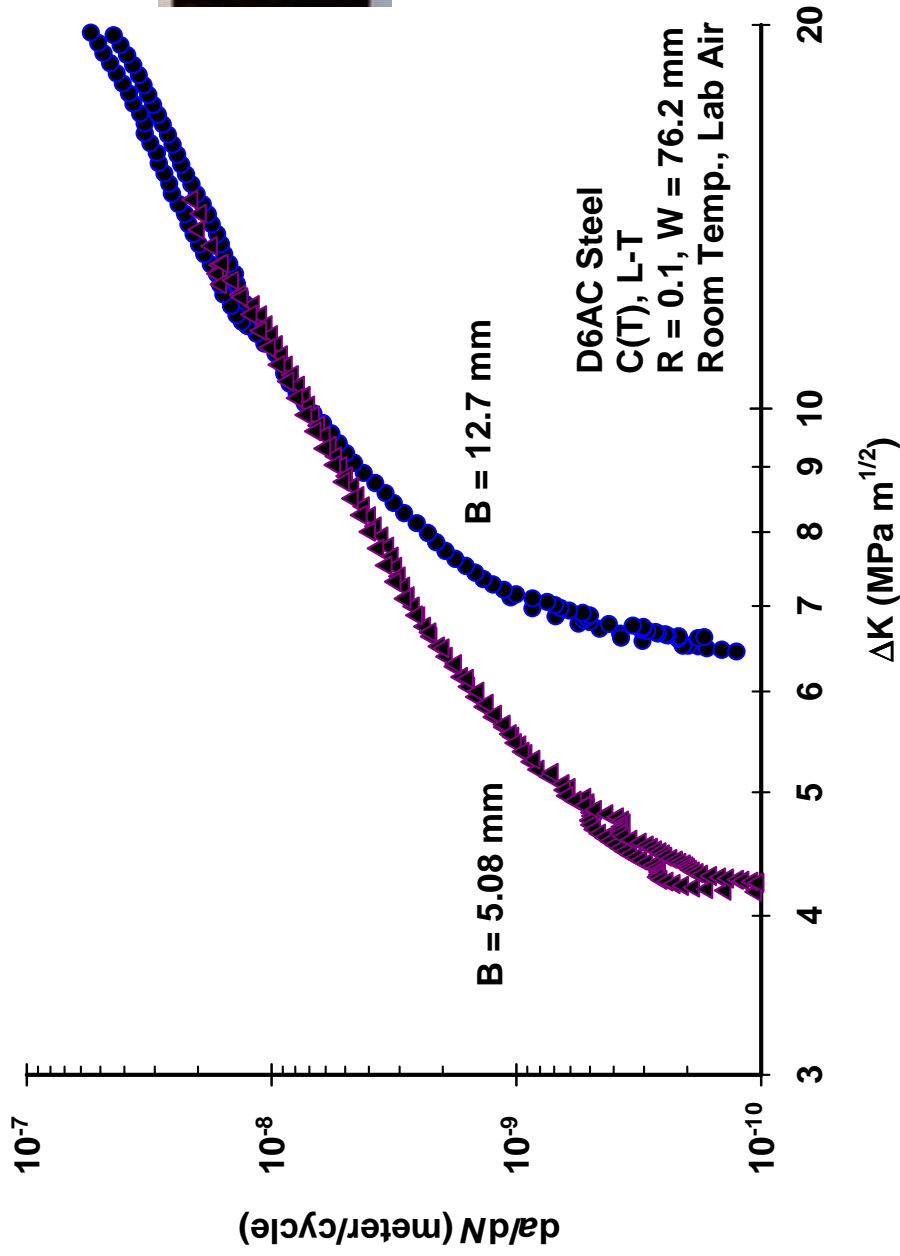


Effect of Laboratory Environment





Specimen Thickness Effects



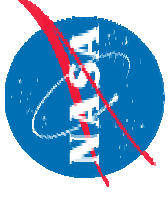
Fretting Debris



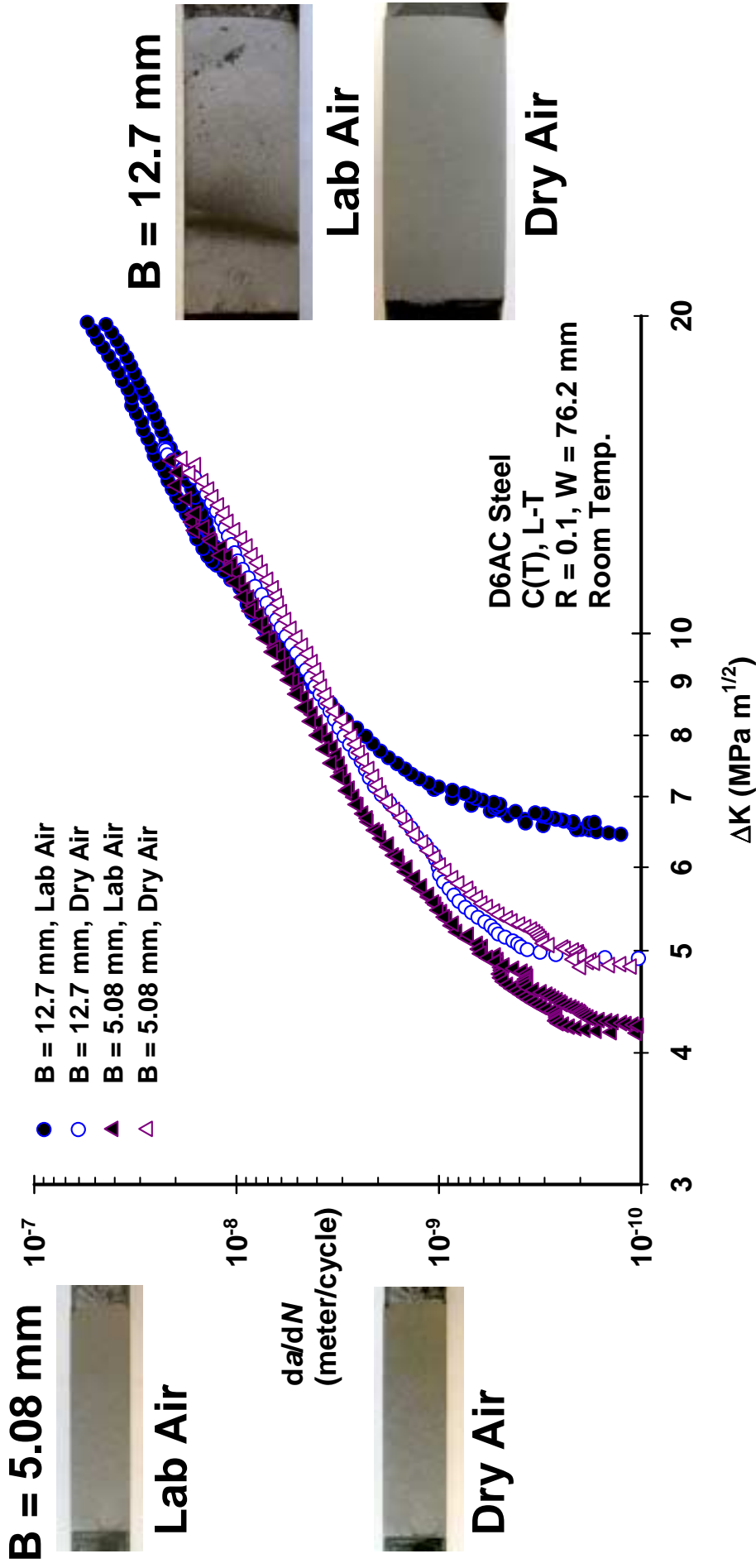
B = 12.7 mm

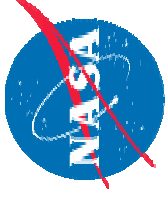


B = 5.08 mm

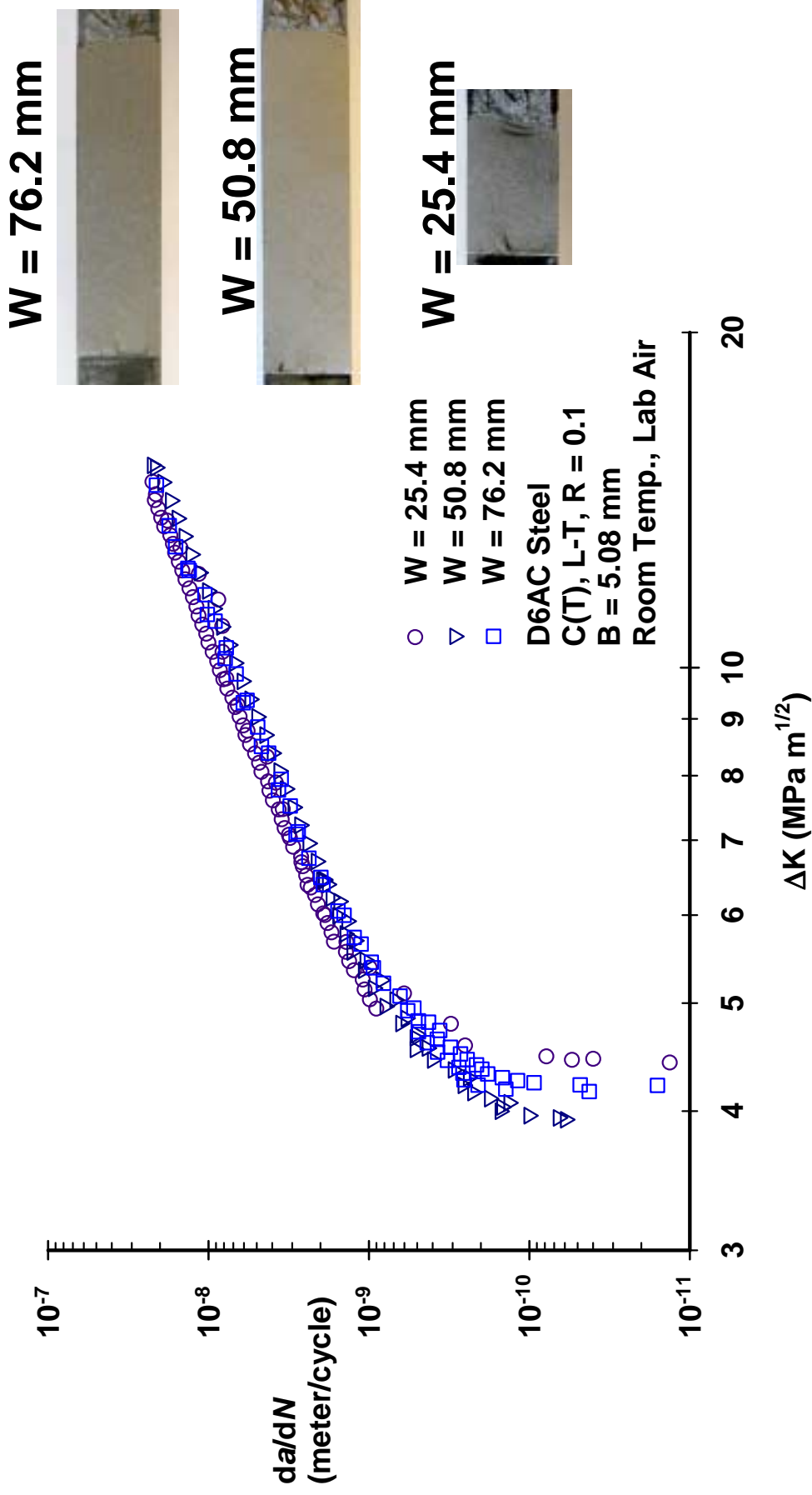


Thickness/Environmental Effects for $W = 76.2$ mm

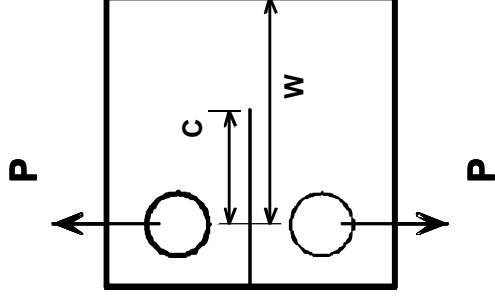
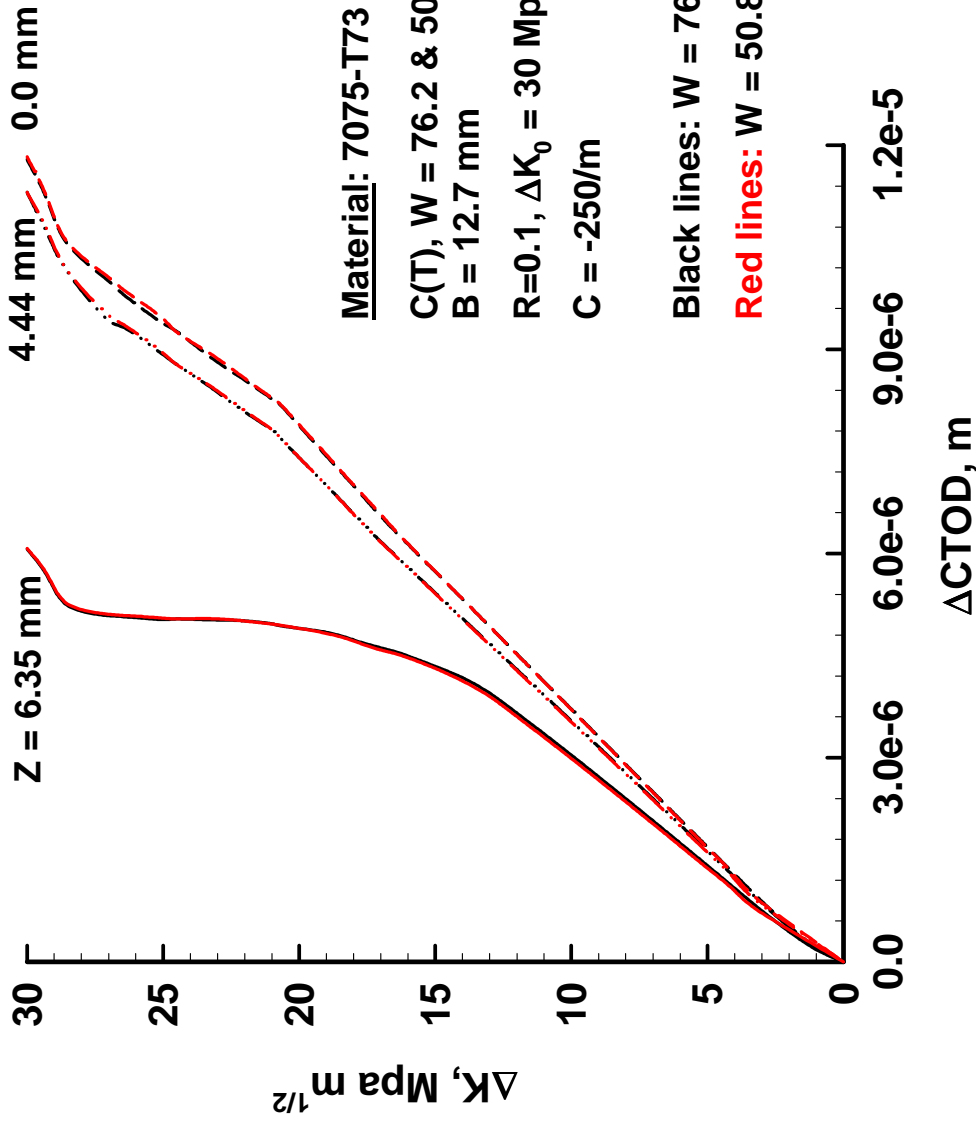
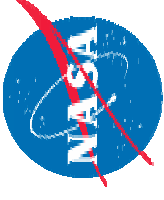


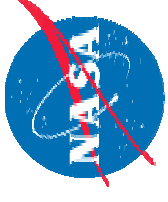


Specimen Width Effects in Lab Air

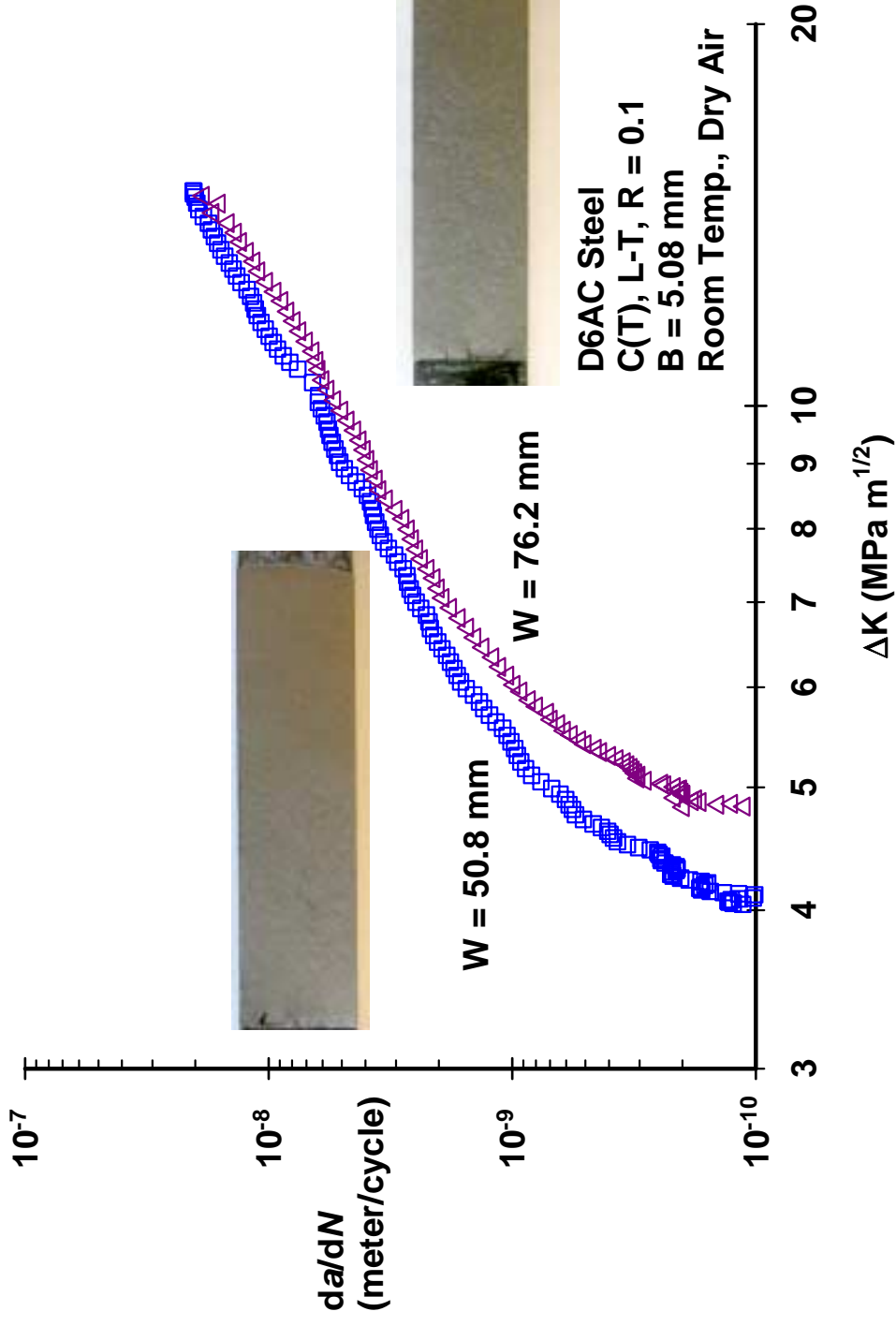


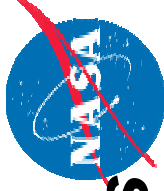
Δ CTOD for Different Width $C(T)$ Specimens



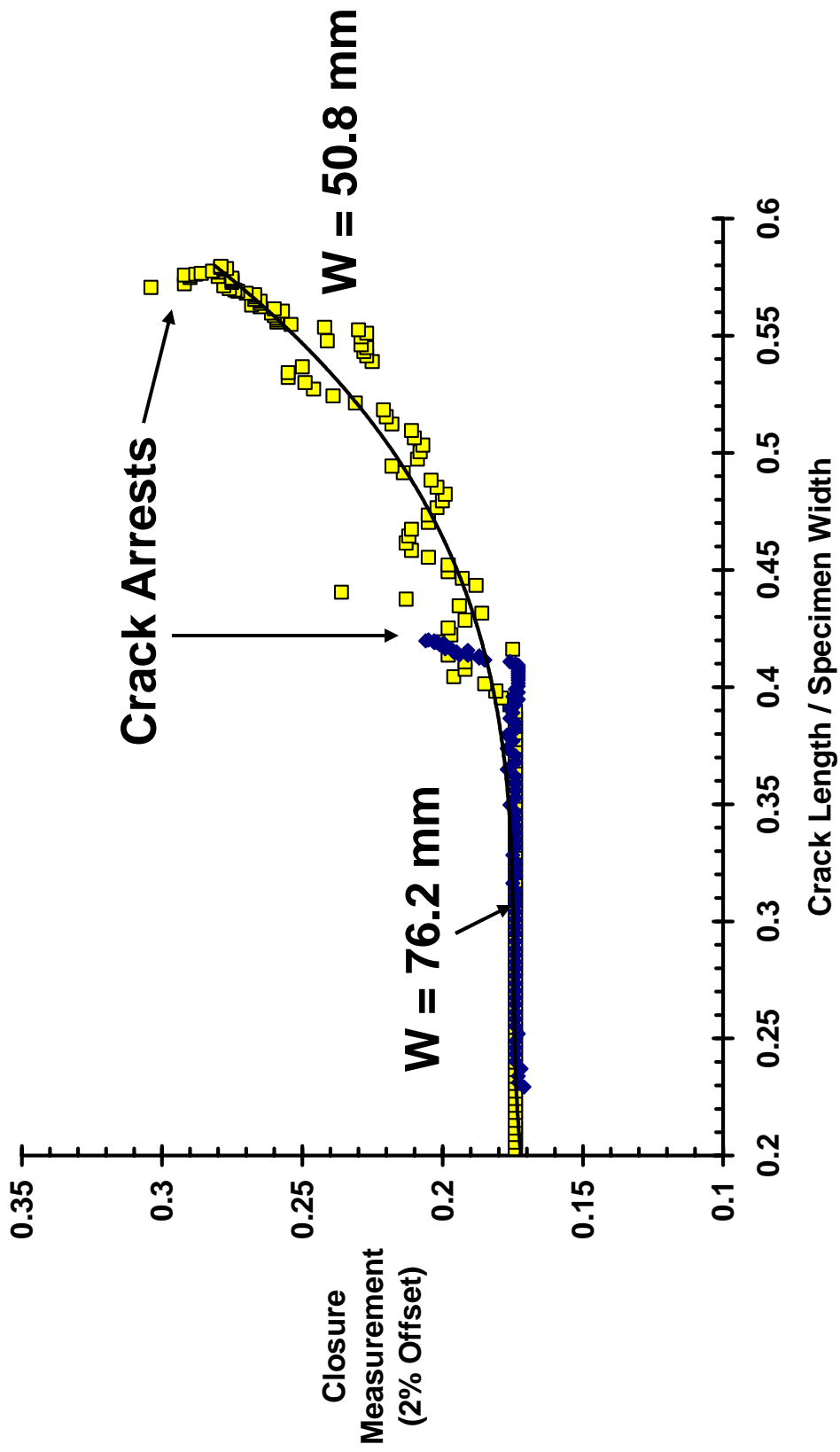


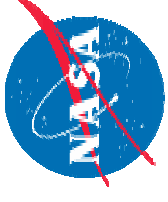
Specimen Width Effects in Dry Air



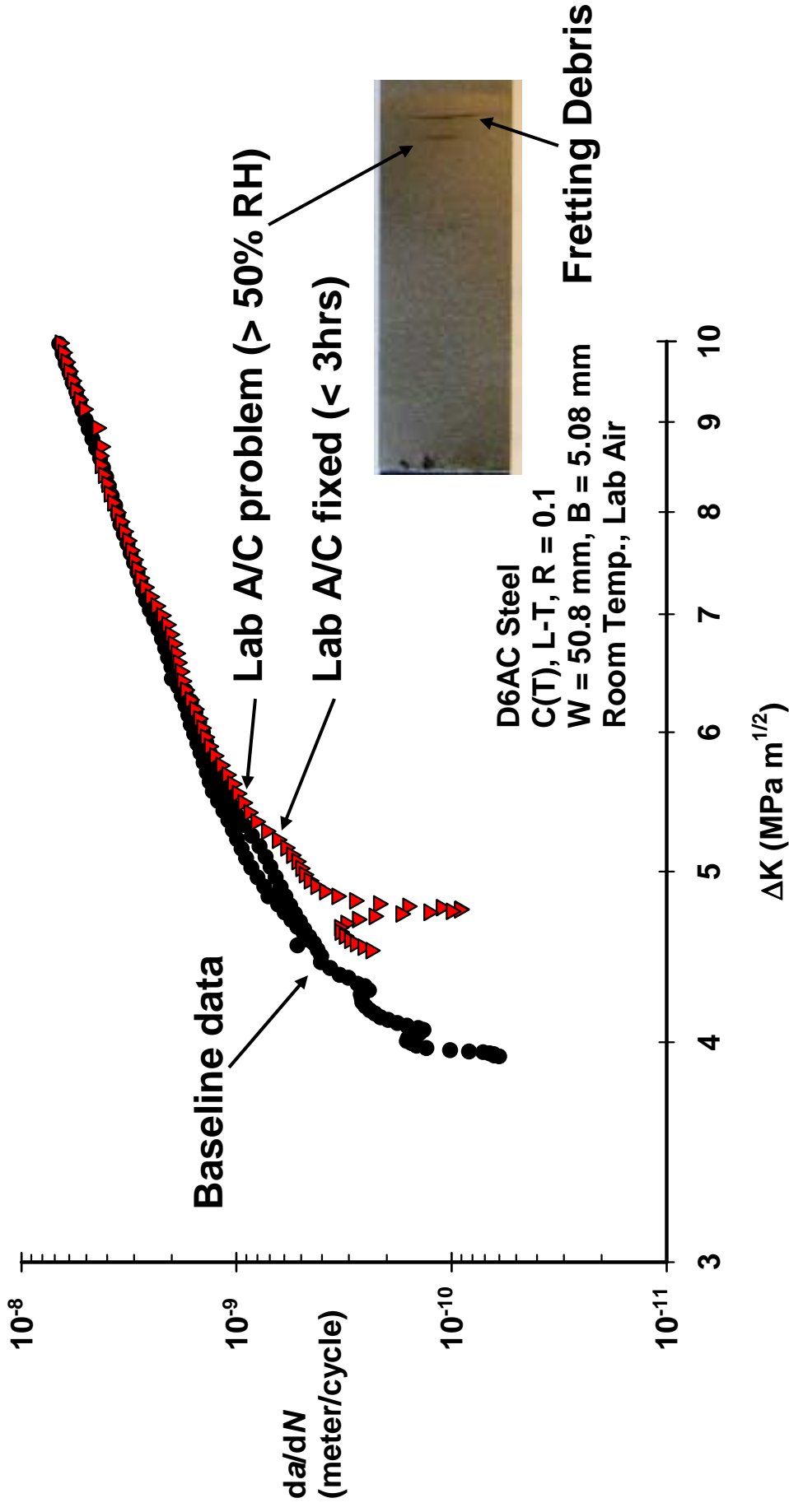


Closure Measurements of Dry Air Tests

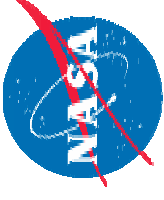




Sensitivity to Humidity



Δ CTOD and closure level for C(T) and M(T) specimens



Material: 7075-T73

W = 76.2 mm

B = 12.7 mm

$K_{max} = 11.1111 \text{ Mpa m}^{1/2}$

$\Delta K_0 = 10 \text{ Mpa m}^{1/2}$

C = -500/m

da = 0.01 mm

R = 0.1

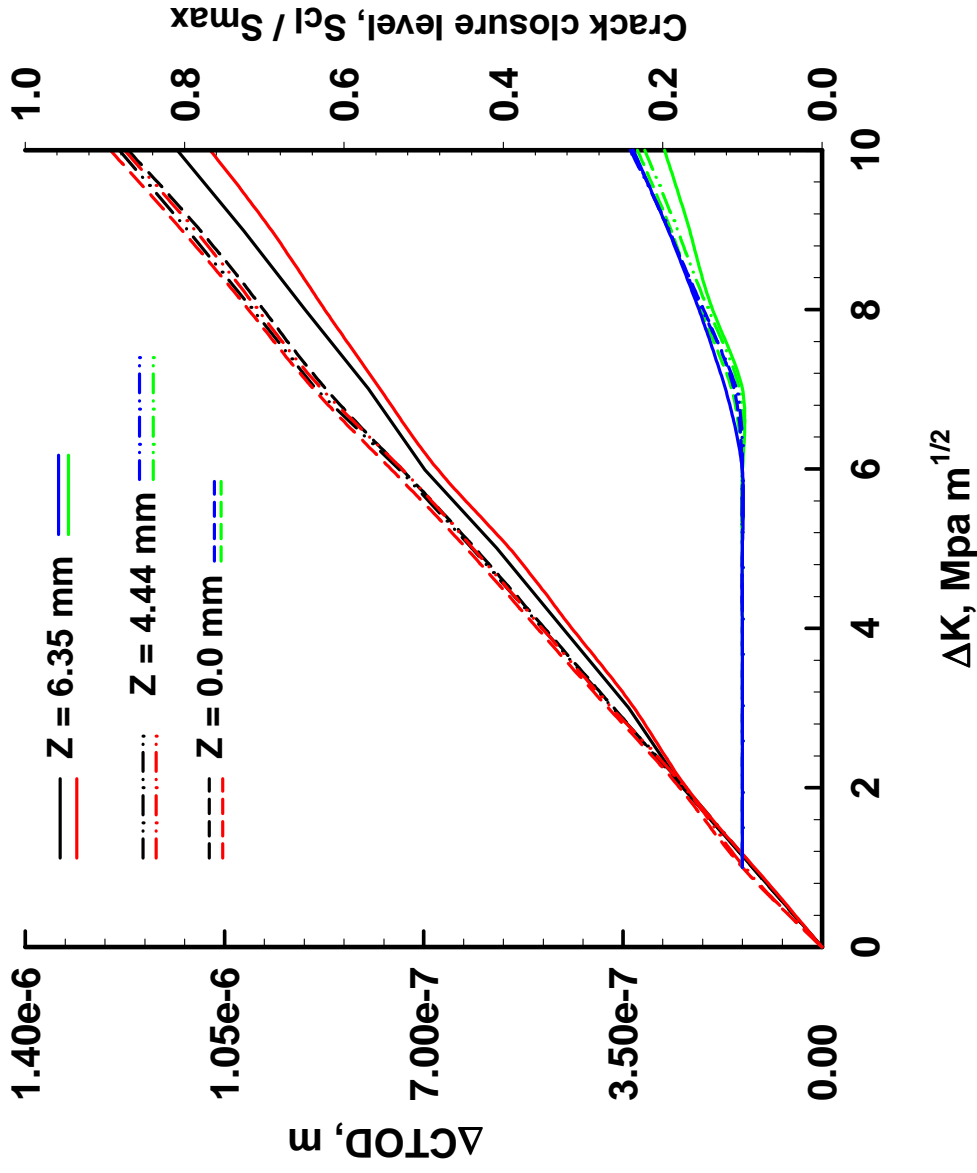
Δ ctod at 0.01 mm

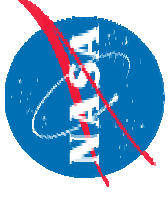
Black lines: M(T)

Red lines: C(T)

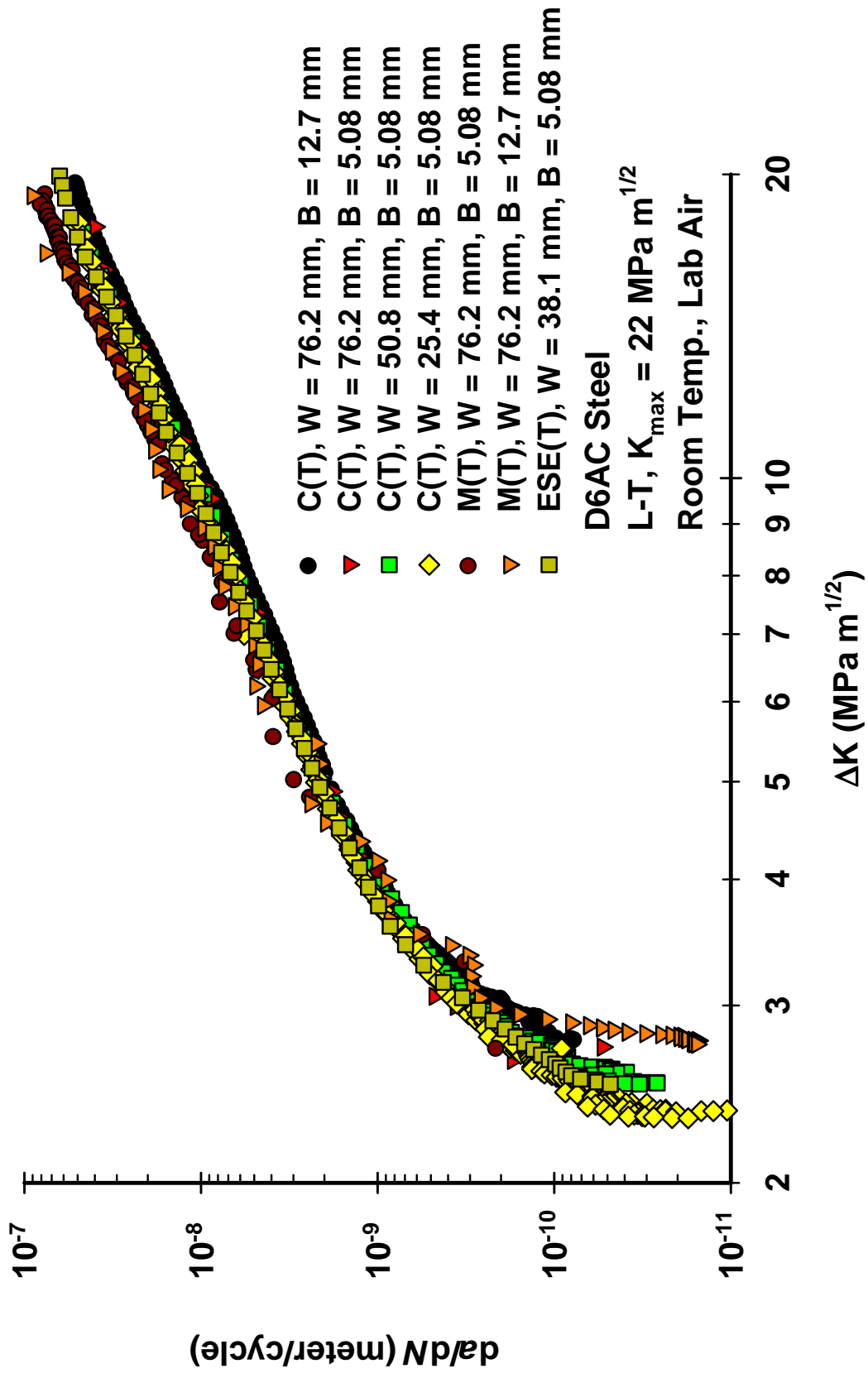
Blue lines: M(T)
(Local crack closure)

Green lines: C(T)
(Local crack closure)

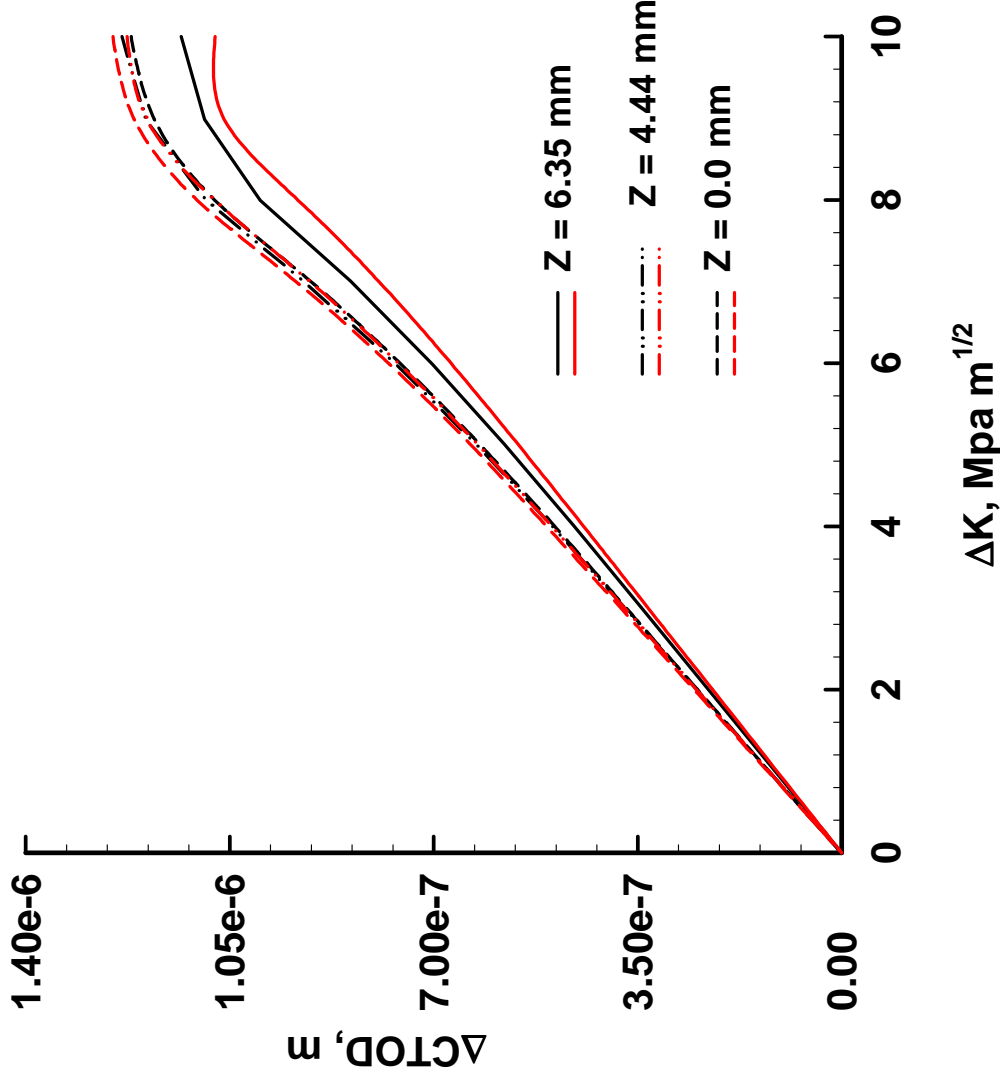
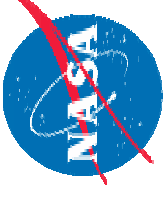




Constant K_{max} Data



Δ CTOD and closure level for C(T) and M(T) specimens



Material: 7075-T73

W = 76.2 mm

B = 12.7 mm

$K_{\max} = 11.1111 \text{ Mpa m}^{1/2}$

$\Delta K_0 = 10 \text{ Mpa m}^{1/2}$

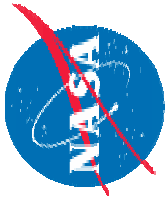
C = -500/m

da = 0.01 mm

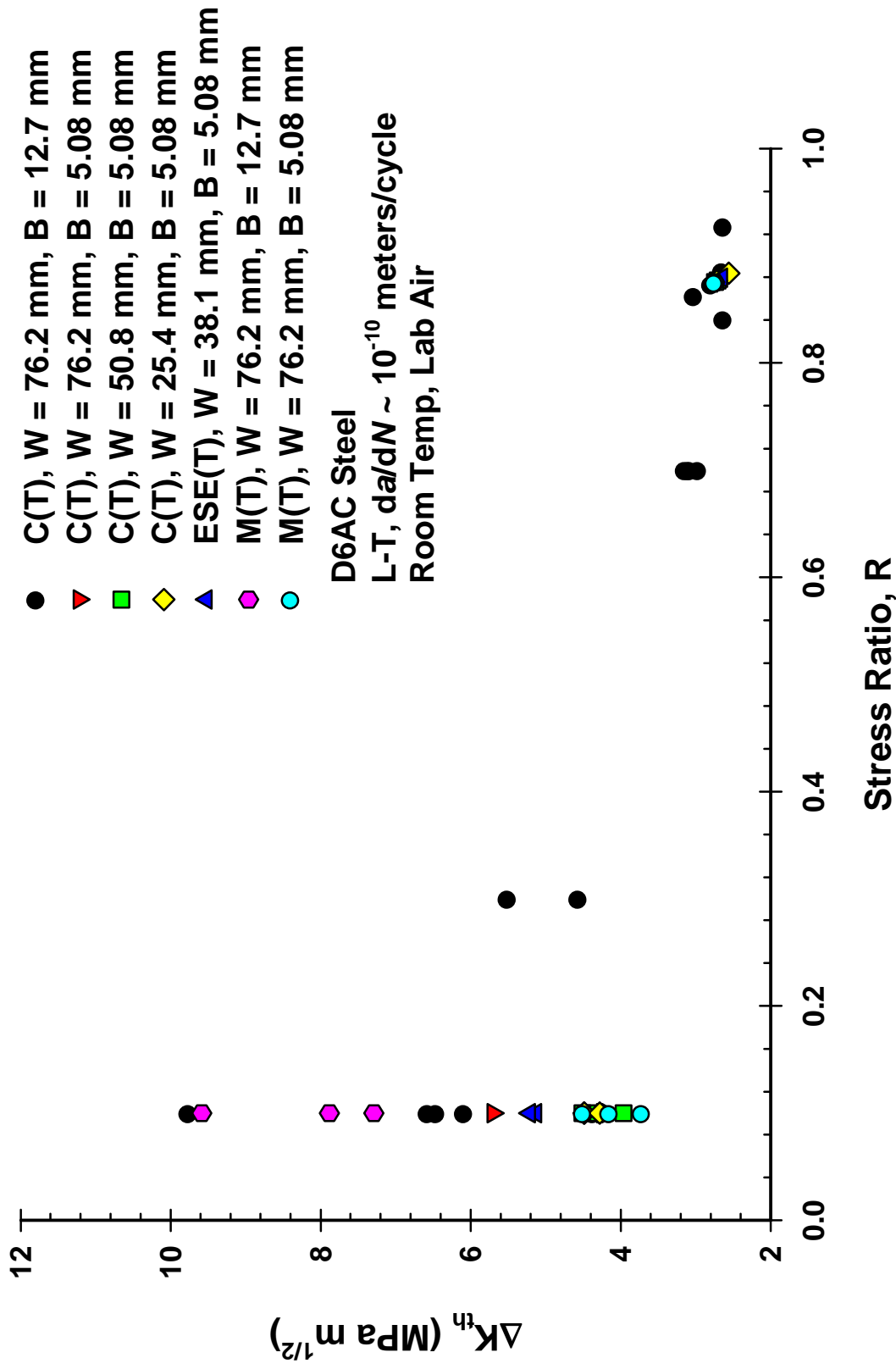
Δ ctod at 0.01 mm

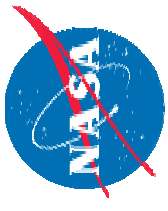
Black lines: M(T)

Red lines: C(T)



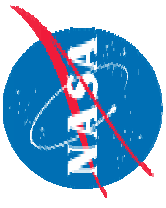
Specimen Configuration Effects at Threshold





Concluding Remarks

- **Analyses predicted remote plasticity-induced crack closure under constant-R load reduction procedure**
- **Test data shows closure affects threshold under constant-R load reduction procedure**
- **Local CTOD estimates for C(T) specimen with different widths compared well with one another.**
- **Cyclic CTOD estimates for M(T) specimen are within the bounds of C(T) specimen.**
- **Test data shows that different width and thickness C(T), M(T) and ESE(T) specimens generate different thresholds**



Planned Work

- Experimental 7075-T73 Aluminum
 - M(T), C(T), ESE(T)
 - Dry Air and Lab Air
- Computational
 - CTOD values for D6AC Steel
- Guidance
 - Develop testing and analysis guidelines for NASA programs